Available online at www.sciencedirect.com
ScienceDirect
Journal of the European Ceramic Society 28 (2008) 61–68
www.elsevier.com/locate/jeurceramsoc

Glass–ceramic seal to join Crofer 22 APU alloy to YSZ ceramic in planar SOFCs

F. Smeacetto [a,*], M. Salvo [a], M. Ferraris [a], J. Cho [b], A.R. Boccaccini [b]

[a] *Department of Materials Science and Chemical Engineering, Politecnico di Torino, Corso Duca degli Abruzzi 24, 10129 Torino, Italy*
[b] *Department of Materials, Imperial College London, Prince Consort Road, London SW7 2BP, UK*

Received 28 February 2007; received in revised form 20 April 2007; accepted 5 May 2007
Available online 12 July 2007

Abstract

This work describes the design and development of a glass–ceramic seal to produce a hermetic joint between the ceramic electrolyte and the metallic interconnect of planar SOFC stacks. The glass–ceramic composition was designed considering the chemical compatibility with the ceramic electrolyte (yttria stabilized zirconia) and the oxidation resistant metal alloy interconnect (Crofer 22 APU), the thermo-mechanical properties (characteristic temperatures, thermal expansion coefficient), and the wettability on the substrates. The designed glass–ceramic seal is a barium-free silica-based glass, which partially crystallizes during the heat treatment after being deposited on Crofer 22 APU substrate by slurry coating or by electrophoretic deposition.

The sealing process of the glass–ceramic was optimized, also taking into account that the maximum processing temperature should be lower that 950 °C (upper limit for the metallic interconnect) and the maximum heating rate of about 5 °C/min (limit for ceramic components). The joined ceramic/seal/metal samples were morphologically characterized and preliminary tested for 400 h in air atmosphere at the fuel cell operating temperature of 800 °C. Thermal ageing in air caused a Cr-diffusion from Crofer 22 APU alloy to the seal only when the alloy was used in the as-received condition. The preoxidised one did not diffuse Cr ions through the seal under the same ageing conditions.

Keywords: Glass–ceramic; Fuel cell; Joining; Interconnect

1. Introduction

Solid oxide fuel cells (SOFCs) are energy conversion devices which produce electricity by the electrochemical reaction between fuel and an oxidant.[1] Among the different SOFCs, the planar type, which is expected to be cost effective and mechanically robust, offers an attractive potential for increased power densities compared to other concepts.[2–5] The repeating unit of a planar configuration is formed by the combination of joint anode–electrolyte–cathode structures and interconnect; the interconnect provides electrical connection between the anode of one individual cell (repeating unit) to the cathode of the neighbouring one.[6] In most planar solid oxide fuel cell stack designs, the interconnect, which is an oxidation resistant alloy (chromia-forming ferritic stainless steels) [7–9] has to be sealed to the adjacent components.

The seal must meet some important requirements: it has to be hermetic, in order to prevent mixing of fuel and oxidant; it should have a thermal expansion coefficient close to those of the interconnect [10] and electrolyte. Moreover, the seal must provide electrical insulation of the cell and it must have low reactivity with the other cell components during the total lifetime of the cell.

In literature, three different approaches are taken in consideration for sealing SOFCs: rigid sealing, compressive sealing, and compliant bonded sealing.[11,12]

By carefully choosing the glass composition, glasses and glass–ceramics meet, in principle, most of the requirements of an ideal sealant.[13–19] Glass–ceramics, which can be prepared by controlled sintering and crystallization of glasses, possess superior mechanical properties and higher viscosity at the SOFC operating temperature than glasses. Furthermore,

* Corresponding author. Tel.: +39 011564706; fax: +39 0115644699.
E-mail address: federico.smeacetto@polito.it (F. Smeacetto).

0955-2219/$ – see front matter © 2007 Elsevier Ltd. All rights reserved.
doi:10.1016/j.jeurceramsoc.2007.05.006

glass–ceramics can have thermal expansion coefficients very different from the parent glass, due to the different crystalline phases and their relative concentration. To develop a suitable glass–ceramic sealant, it is therefore necessary to understand crystallization kinetics, sealing properties and chemical interaction when in contact with other components of the cell. For example, barium aluminosilicate sealants have shown high reactivity with the metallic interconnect at 800–900 °C forming a porous and weak interface composed of barium chromate ($BaCrO_4$) and monocelsian ($BaAl_2Si_2O_8$)[15,17,18] while phosphate and borate glasses are not sufficiently stable in a humidified fuel gas environment.[21]

In this study, a barium- and boron-free glass–ceramic was chosen to join Crofer 22 APU alloy to an yttria stabilized zirconia wafer. The same glass–ceramic was used for electrophoretic deposition of a sealant layer on as-received Crofer 22 APU foils.

2. Experimental

The heat resistant metal alloy used for this study was Crofer 22 APU (manufactured by Tyssen Krupp, Germany and supplied by HT Ceramix, Switzerland), which is a ferritic stainless steel containing 22 wt.% chromium and exhibits a thermal expansion coefficient of $11.5 \times 10^{-6}\ K^{-1}$. The yttria 8 mol% zirconia wafer (with a thermal expansion coefficient of $10.5 \times 10^{-6}\ K^{-1}$) had a thickness of 200 μm and was supplied by HT Ceramix (Switzerland). Crofer 22 APU and YSZ samples to be joined were cut to dimensions: 10 mm × 8 mm × 2 mm.

A glass–ceramic sealant based on the system SiO_2, Al_2O_3, CaO, and Na_2O was designed, produced and tested. The sealant composition ranged between 50 and 55 wt.% SiO_2, 10 and 12 wt.% Al_2O_3, 20 and 23 wt.% CaO, and 10 and 12 wt.% Na_2O.

The sealant, labelled as SACN, was produced as a glass by melting the appropriate raw materials in different proportions and by heating at 1500 °C for 1 h in a platinum crucible; the melt was cast on a metal plate and the transparent glass was ground for differential thermal analysis (DTA) (Perkin Elmer DTA7) and hot stage microscopy experiments (Leitz GmbHAII).

The glass was powdered and sieved into four different size ranges: <38, 38–75, 75–106 and >106 μm. The particle size for each fraction was used for analyzing the thermal behaviour of the glass power as a function of the particle size by DTA. DTA scans were recorded from room temperature to 1000 °C in flowing dry argon at various heating rates (5, 10 and 25 °C/min). Coefficients of thermal expansion were measured on SACN bars (8 mm × 5 mm × 4 mm) in a Perkin Elmer Thermomechanical Analyser, TMA (heating rate 5 °C/min).

Studies of wettability of SACN glass on Crofer 22 APU alloy (as received and preoxidised at 950 °C in air for 2 h, 25 °C/min) and on YSZ ceramic were carried out by heating microscopy (Leitz Wetzlar, Germany) or in a tubular oven under air or Ar atmosphere. The SACN glass powders (<38, 38–75, 75–106 and >106 μm) were deposited on Crofer 22 APU samples by slurry coating, heated and observed by optical microscopy and SEM.

Joined Crofer 22/SACN/YSZ samples were obtained by sandwiching the SACN glass (<38 to <75 μm) coated YSZ wafer and the Crofer 22 APU plate. Heat treatment was performed in a tubular oven (Ar atmosphere) at a temperature above the glass softening point, without applying any load. The joining thermal treatment was carried out from room temperature to 900 °C with a dwelling time of 30–120 min at 900 °C and a heating rate of 5 or 25 °C/min.

The crystalline phase composition of the sealing material after heat treatment was determined by X-ray diffraction (XRD) analysis.

Glass pellets from SACN powder (<38 to <75 μm) were sintered at 900 °C with a dwelling time of 30 min (25 °C/min heating rate); the resulting glass–ceramic bar was used in the TMA apparatus for measuring the coefficient of thermal expansion. Some glass–ceramic bars were thermal aged at 800 °C for 400 h in air: the coefficient of thermal expansion of the aged glass–ceramic was measured by TMA and the crystal phase composition by X-ray diffraction analysis.

The joined samples (sandwich structure) were morphologically characterized by SEM observations. Preliminary EDS analysis was carried out in order to asses chromium diffusion into the seal both before and after thermal ageing at 800 °C for 400 h in air.

In an attempt to provide more control of the thickness and uniformity of the glass–ceramic layer, SACN glass powders (<38 μm) were also deposited on Crofer 22 APU substrate by EPD. Aqueous suspensions containing different wt.% of glass powder were prepared; all suspensions were dispersed ultrasonically and subsequently deposited on the Crofer 22 APU substrate. The experimental details of EPD of glass powders from aqueous suspensions are similar to those reported elsewhere.[20] The EPD parameters (concentration of glass powder in aqueous suspensions, applied voltage, and deposition time) were optimized by trial-and-error in order to obtain a dense layer of controlled thickness of SACN glass on Crofer 22 APU substrates.

3. Results and discussion

3.1. Sealant characterization

The sealant composition was chosen in order to obtain a glass with adequate characteristic temperatures and thermal expansion coefficient (these values were calculated by SciGlass software) and to avoid the use of BaO and B_2O_3, which are undesired in this application as described in Section 1.

Table 1 shows the characteristic temperatures for the SACN system: since the softening point of the glass is about 740 °C, the joining process was carried out below 950 °C (the upper temperature for the Crofer 22 APU alloy). TMA measurements revealed a thermal expansion coefficient of the as produced SACN glass of $(9.4–9.8) \times 10^{-6}\ °C^{-1}$ (300–500 °C).

Table 1
Thermomechanical properties of the sealant material (SACN glass)

	SACN glass
Glass transition temperature (°C)	670
Softening temperature (°C)	740
Thermal expansion coefficient	$(9.4–9.8) \times 10^{-6}\ °C^{-1}$ (300–500 °C)

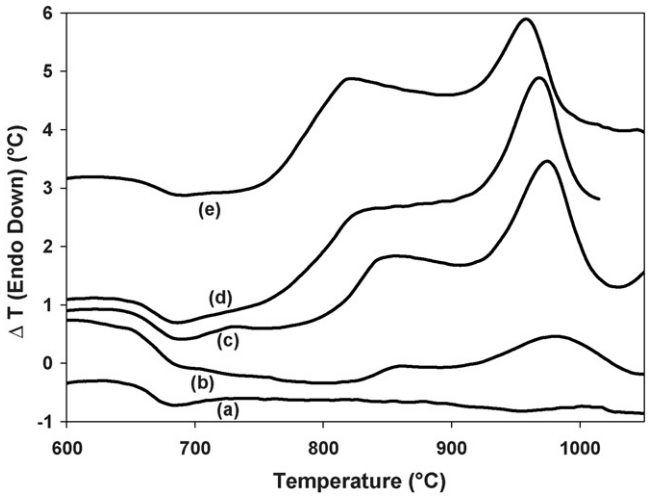

Fig. 1. DTA analysis of SACN glass powders sieved at five different mean size (d) ranges (heating rate 25 °C/min); curve (a) bulk glass, curve (b) $d > 106$ μm, curve (c) 75 μm $< d <$ 106 μm, curve (d) 38 μm $< d <$ 75 μm, and curve (e) $d <$ 38 μm.

Fig. 1 shows the DTA curves (heating rate 25 °C/min) of SACN powders sieved at four different mean particle size ranges and of SACN bulk glass. The T_g is found to be at 670 °C and two exothermic peaks can be detected at higher temperatures. The two peaks are considerably affected by the particle size; both these peaks are shifted to lower temperatures when decreasing the particle size, suggesting a possible effect associated with surface crystallization of the glass.[22,23] A decrease in the second crystallization peak height with increasing particle size can be observed; this behaviour also suggests that the crystalline phase formation starts mainly on the surface of the glass particles.

Fig. 2 shows DTA curves for different heating rates (particle size 38–75 μm). It is observed that the crystallisation peaks shifted to higher temperatures with increasing heating rate.

The energy of crystallisation, E_c, for the two peaks was estimated by the Kissinger equation [24]:

$$\ln\left(\frac{\phi}{T_P^2}\right) = -\frac{E_c}{RT} + \text{const.} \quad (1)$$

Where ϕ is the heating rate, R the gas constant and T_P is the crystallisation peak temperature. A plot of $\ln(\phi/T_P^2)$ versus $1/T_P$ is a straight line, whose slope corresponds to E_c. The activation energies for the first and second crystallisation phenomena were found to be 380 and 255 kJ/mol, respectively.

Fig. 3a and b shows the XRD spectra of SACN glass–ceramic samples heated at 5 °C/min up to 800 and 900 °C with a dwelling time of 30 min, respectively. In the XRD pattern of Fig. 3a only the $Ca_2Al_2SiO_7$ phase was detected, together with the presence of an amorphous halo, evidence of a residual glassy phase; the formation of this crystalline phase was assigned to the exothermic peak around 800 °C, reported in Fig. 2, curve a. The XRD pattern of Fig. 3b shows the formation of different crystalline phases, i.e. $Ca_2Al_2SiO_7$ and $NaAlSiO_4$. Thus the second DTA exothermic peak (around 900 °C) was assigned to the $NaAlSiO_4$ formation.

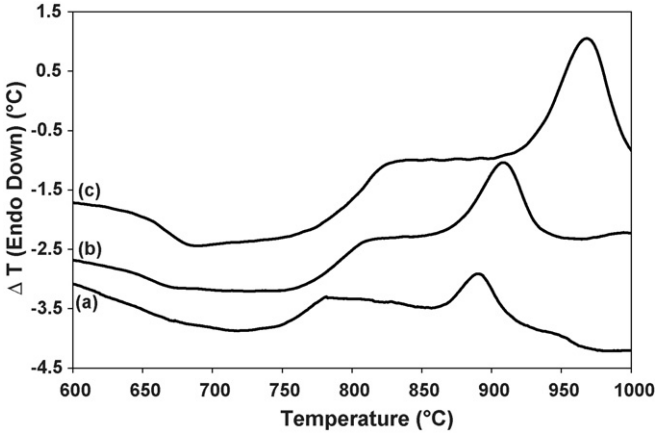

Fig. 2. DTA analysis of SACN powder (38 μm $< d <$ 75 μm) at different heating rates: (a) 5 °C/min; (b) 10 °C/min and (c) 25 °C/min.

TMA measurements on a SACN glass pellet sintered at 900 °C for 30 min revealed a thermal expansion coefficient of 10.7×10^{-6} °C^{-1}. Crystallization of the glass resulted in an increase of the thermal expansion coefficient, but still the value is intermediate between those of Crofer 22 APU alloy and YSZ ceramic, as required for this application.

3.2. Hot stage microscopy and wettability

Preliminary compatibility tests between the SACN glass–ceramic seal and preoxidised Crofer 22 APU alloy, and SACN glass–ceramic seal and YSZ ceramic were conducted in a hot-stage microscope using different powder sizes (<20, 20–38, 38–75, 75–106 and >106 μm) (25 °C/min, Ar).

Except in one case, with SACN glass particles <20 μm, where the Crofer 22 APU alloy was wetted but only partially coated, in the other cases the wettability on both substrates was outstanding (Fig. 4), which is thought to be due to a lack of glass formation.

Nevertheless, a slight increase in porosity was observed by decreasing the glass particle size from >106 to 20–38 μm (pictures not reported here), as expected due to the occurrence of sintering with concurrent surface induced crystallization, as discussed in Section 3.1.

Moreover, the X-ray diffraction analysis revealed that an almost complete crystallisation of the glass could be achieved after 30 min at 900 °C only with powders of mean particle size <75 μm. This behaviour is probably due to the fact that surface induced crystallization of glass powders >75 μm should lead only to partial crystallisation.

As discussed above, a high degree of crystallisation is needed to increase thermo-mechanical properties of the sealant and to prevent microstructural modification during SOFC operation at high temperatures (up to 900 °C). In this regard, the best compromise between residual porosity and degree of crystallisation was obtained using SACN glass powder with average particle size in the range 38–75 μm and heat treatment at temperatures of 900 °C for 30 min.

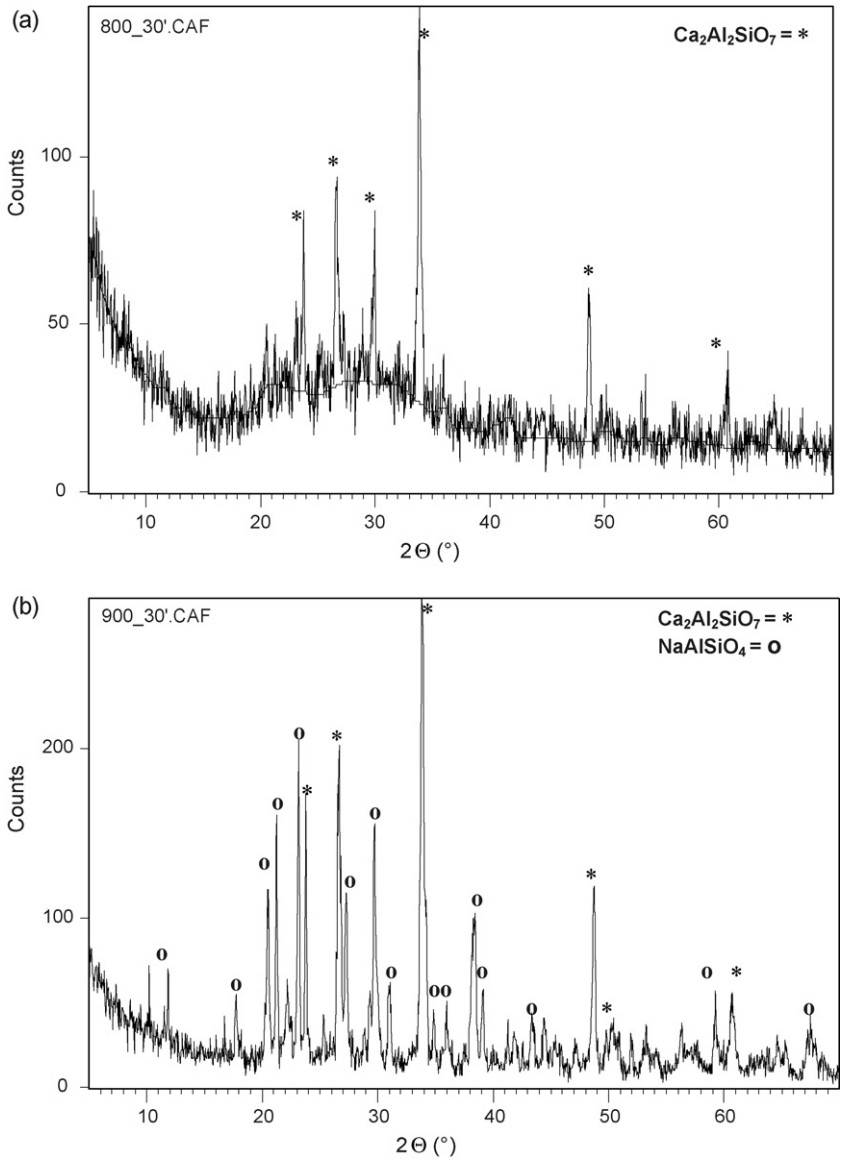

Fig. 3. (a) XRD measurements conducted on the silicate seal (after heat treatment at 800 °C with a dwelling time of 30 min, heating rate 5 °C/min). (b) XRD measurements conducted on the silicate seal (after heat treatment at 900 °C with a dwelling time of 30 min, heating rate 5 °C/min).

3.3. EPD deposition and heat treatment

The SACN glass particles in distilled water were negatively charged and moved towards the anode under the applied field. By a trial-and-error approach varying the EPD parameters, as explained elsewhere,[20] the optimal suspension concentration, voltage and deposition time, were determined. The best results in terms of uniformity of the glass deposits were achieved with suspensions of distilled water containing 20 wt.% glass, applied voltage of 5 V and deposition time of 5 min, with continuous magnetic stirring. The deposits were dried at room temperature for 24 h.

Fig. 5a shows a SEM micrograph of the cross-section of a SACN glass layer as deposited on Crofer 22 APU substrate by EPD. It can be seen that the SACN glass coating has a fairly uniform thickness of approximately 40 μm. Thicker layers could be

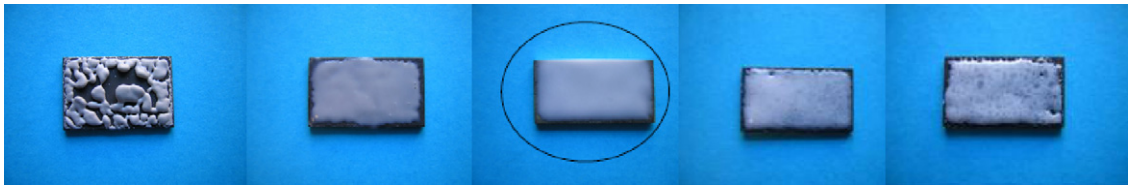

Fig. 4. Wettability of SACN glass on Crofer 22 APU using different SACN powder sizes ($d < 20$ μm, $d = 20$–38 μm, $d = 38$–75 μm, $d = 75$–106 μm and $d > 106$ μm) (25 °C/min, Ar).

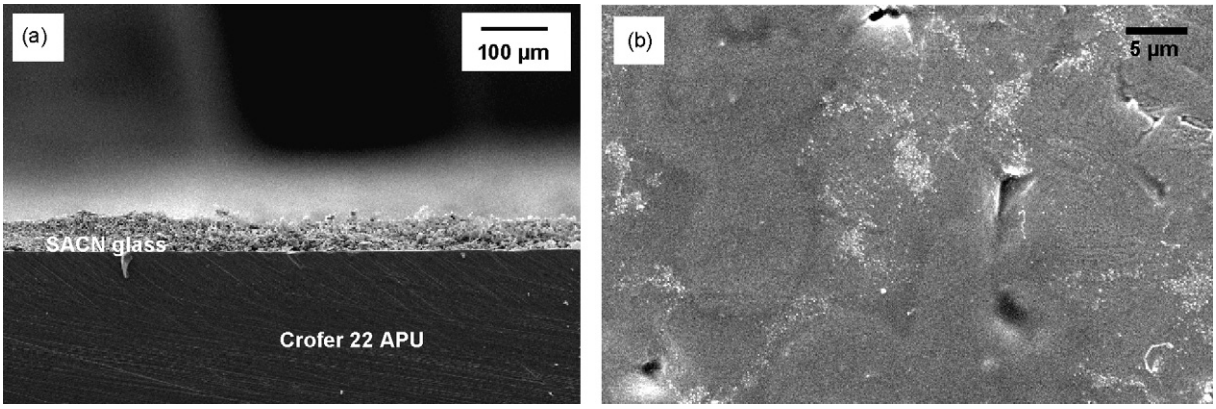

Fig. 5. (a) Cross-section of SACN glass deposited on Crofer 22 APU substrate by EPD. Conditions: 20 wt.% five glass in suspension, applied voltage 5 V and a deposition time 5 min. (b) SEM top view of a sintered layer of glass sealant deposited by EPD.

obtained, if required, by modifying EPD parameters, as shown elsewhere for other silicate glass systems.[20] The EPD layers were sintered by the same thermal treatment used for the slurry-based samples, i.e. Ar atmosphere with a dwelling time of 30 min at 900 °C and heating rate of 5 or 25 °C/min. Fig. 5b shows the obtained result: the Crofer 22 APU substrate is seen to be uniformly coated by the EPD glass–ceramic layer.

3.4. Preparation and characterization of joined samples

Accordingly to what was discussed above, SACN glass powders (38–75 μm) were deposited on as received and pre-oxidised Crofer 22 APU substrates by both slurry coating technique and EPD. Then as received and preoxidised Crofer 22 APU/SACN/YSZ joined samples were prepared with a "sandwich like" structure. At the sealing temperature of 900 °C no differences in the joining porosity and crystalline structure were observed by increasing the dwelling time from 30 to 120 min. Although EPD provided a better control of the thickness of the seal layer, no major difference was expected regarding the structural integrity of the sandwich structure developed by both methods. Therefore the further characterisation was concentrated on the structures made by slurry deposition.

The SACN glass–ceramic interfaces with both as received and preoxidised (not reported here) Crofer 22 APU alloy and YSZ ceramic are continuous, no cracks are present and the glass–ceramic sealant exhibits a fairly homogeneous microstructure (Fig. 6).

Moreover Fig. 7 shows the cross-section of a Crofer 22 APU/SACN/YSZ joined sample obtained at 900 °C (heating rate 25 °C/min, dwelling time 30 min), where residual porosity is observed in the sealant.

The influence of heating rate on the glass–ceramic sintering behaviour and on the sealant residual porosity was investigated on as received and preoxidised Crofer 22 APU/SACN/YSZ joined structures. The cross-section of a joined sample obtained at 900 °C (dwelling time of 30 min) using a heating rate of 5 °C/min is showed in Fig. 8. Very low closed porosity can be now observed in the seal region, thus indicating that this sealant will provide high gas tightness and a hermetic structure. SEM

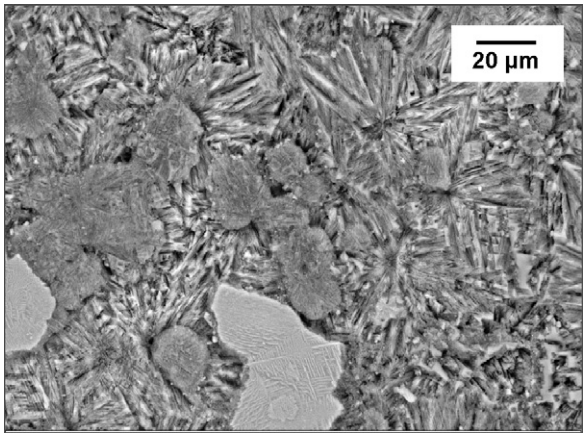

Fig. 6. Glass–ceramic microstructure of the sintered sealant (900 °C, 25 °C/min, 30 min) after HF etching.

images at higher magnification of Crofer 22 APU/SACN and YSZ/SACN interfaces are shown in Figs. 9 and 10, respectively; both interfaces are seen to be continuous and defect free.

The observed decrease in porosity when heating rate decreases (from 25 to 5 °C/min) is probably due to the more effective removal of the gases entrapped in the sealant, during the longer heat treatment. In the literature, it has been frequently

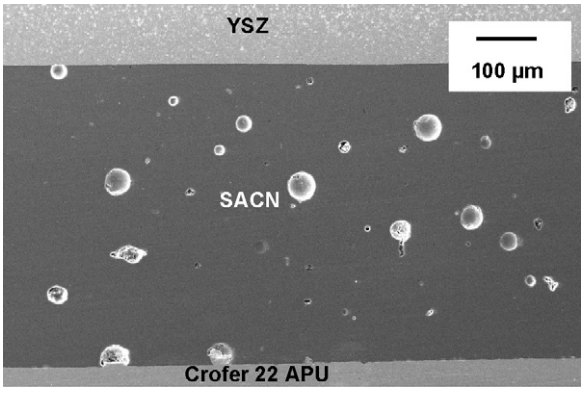

Fig. 7. Cross-section of Crofer 22 APU/SACN/YSZ joined structure obtained at 900 °C (heating rate 25 °C/min) showing residual porosity in the glass–ceramic sealant.

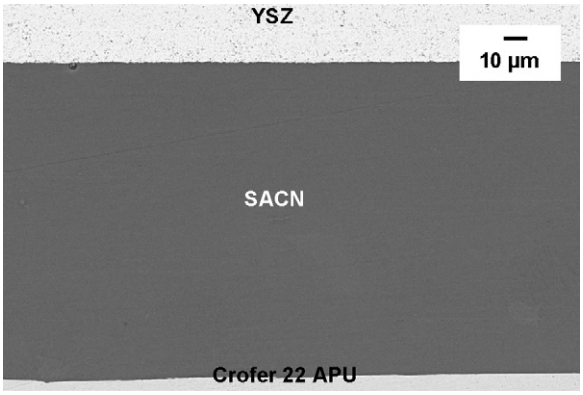

Fig. 8. Crofer 22 APU/SACN/YSZ cross-section obtained at 900 °C (heating rate 5 °C/min).

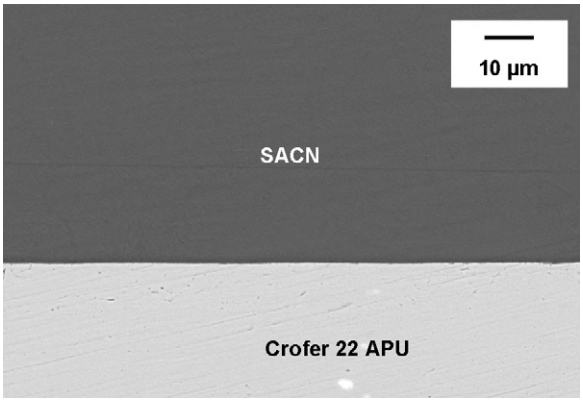

Fig. 9. Cross-section of the interface between Crofer 22 APU alloy and SACN glass–ceramic (heat treatment 5 °C/min, 900 °C, 30 min).

reported that in sintering with concurrent crystallization of glass powders, the heating rate plays a very important role in determining the final product microstructure and properties. The observed behaviour reported in literatures (e.g. [25,26]), however, is generally the opposite to the results of this study, since higher heating rates are reported to overcome concurrent crystallization.[25,26] In our glass–ceramic system, the particle boundaries are not evident and pores approach spherical shape (Fig. 7), which indicates that residual porosity could be determined by bubble formation due to the release of dissolved gas and insoluble gases (e.g. water vapour and air) entrapped in the initial pores. On the other hand, if the heating rate is lower the gases can effectively escape from the joint region when the glass sealant phase viscosity is sufficiently low.

The cross-section of as-joined samples was investigated by SEM–EDS measurements in order to detect possible chromium diffusion from the Crofer 22 APU alloy into the glass–ceramic sealant. However EDS analysis on the as prepared joined samples did not reveal any chromium diffusion into the seal (both for preoxidised and not preoxidised Crofer 22 APU samples) during the joining heat treatment.

Thermal ageing tests in air atmosphere at 800 °C for 400 h were performed on the sealed samples. Fig. 11 shows the cross-section of a Crofer 22 APU/SACN/YSZ joined sample (produced at 900°, heating rate 5 °C/min, dwelling time 30 min), after thermal ageing. It can be observed that the joint region does not exhibit substantial modifications from the morphological point of view; no cracks or pores are present, and the interfaces between the SACN glass–ceramic and both Crofer 22 APU alloy and YSZ ceramic are still continuous and free of cracks.

EDS mapping results are shown in Fig. 12a and b. The Cr EDS mapping at the interface between the SACN glass–ceramic layer and Crofer 22 APU alloy (preoxidised and not preoxidised, before the joining processing) gave different results. As it can be seen in Fig. 12b, Cr diffusion occurs into the SACN glass–ceramic layer for the non-preoxidised Crofer 22 APU/SACN/YSZ joined sample for a depth of about 30 μm from the interface. On the other hand, for the preoxidised Crofer 22 APU/SACN/YSZ joined samples, Cr is not detected in the SACN glass–ceramic layer (Fig. 12a). The preoxidised layer on the Crofer 22 APU alloy substrate (about 1 micron thickness) seems to have acted as a barrier to the Cr diffusion into the SACN glass–ceramic, after 400 h in air at 800 °C.

Finally, it should be noted that the coefficient of thermal expansion of the glass–ceramic, measured by TMA, and the crystal phase composition, detected by XRD, did not change

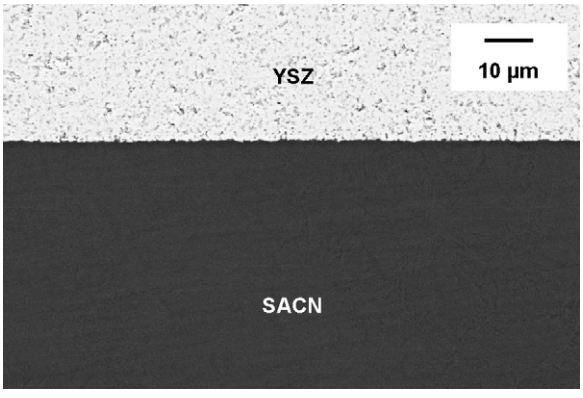

Fig. 10. Cross-section of the interface between YSZ ceramic and SACN glass–ceramic (heat treatment 5 °C/min, 900 °C, 30 min).

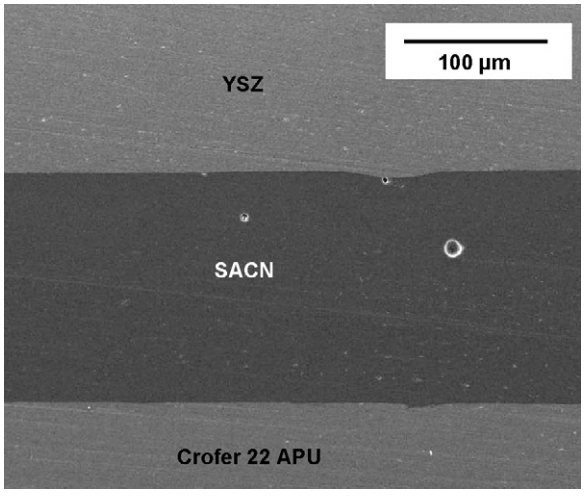

Fig. 11. Cross-section of Crofer 22 APU/SACN/YSZ joined structure obtained at 900 °C (heating rate 5 °C/min), after 400 h of exposure in air at 800 °C.

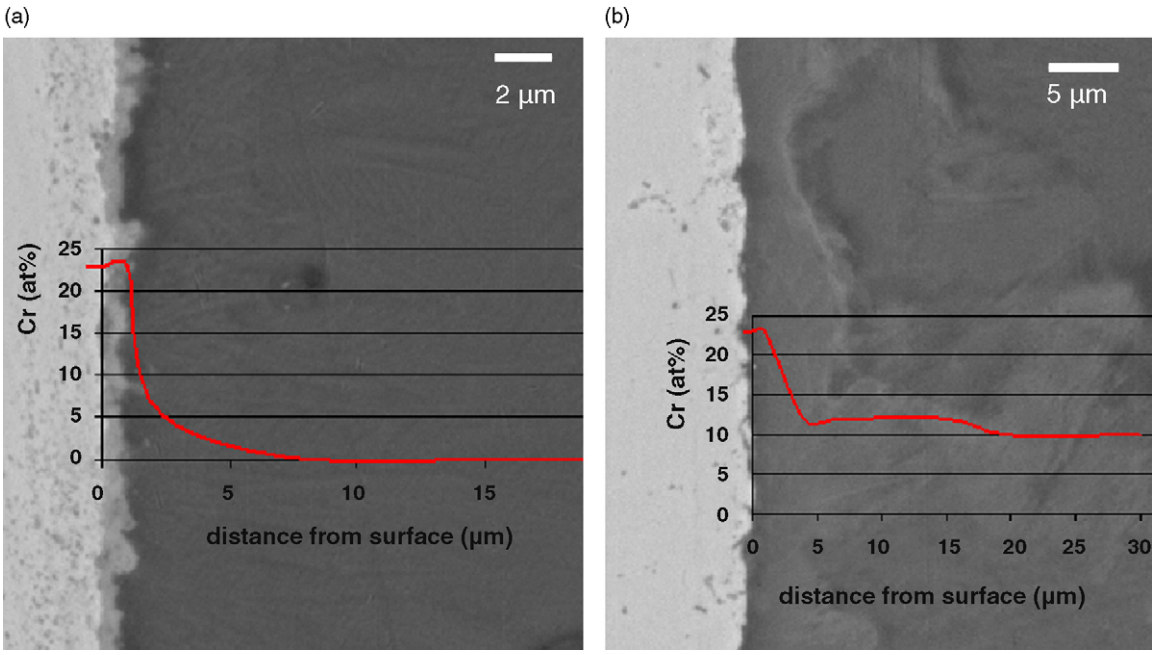

Fig. 12. Cr EDS mapping at the interface between SACN glass–ceramic and Crofer 22 APU substrate after 400 h of exposure in air at 800 °C: (a) preoxidised Crofer 22 APU/SACN interface and (b) not preoxidised Crofer 22/SACN interface.

after thermal ageing, thus indicating the thermo-mechanical stability of the glass–ceramic seal after 400 h at 800 °C in air.

Current investigations focus on the study of the thermal stability of the joined structures in dual atmosphere (air and H_2–3%H_2O).

4. Conclusions

A new barium- and boron-free glass has been designed and successfully used to join YSZ to Crofer 22 APU alloy. The pressure less joining process at 900 °C causes the partial surface induced crystallization of the glass, resulting in a glass–ceramic seal, still having a matched TEC with both YSZ and Crofer 22 APU alloy. The wettability of the seal was determined to be very good on both YSZ and as received- and preoxidised Crofer 22 APU substrates. The powdered glass was successfully applied as a sealant by both slurry coating and by EPD, in air or Ar. The use of EPD can be advantageous for a better control of the glass–ceramic seal thickness. Thermal ageing in air (800 °C, 400 h) caused a Cr-diffusion from Crofer 22 APU alloy to the seal only when the alloy is in the as received condition, whereas the preoxidised one did not result in migration of Cr ions through the seal.

Acknowledgements

The authors gratefully acknowledge Dr. Tagliaferri (HTCeramix) for supplying the interconnect and electrolyte materials, and Miss A. Engert for her useful experimental work.

This work was supported in part by the EU Network of Excellence project Knowledge-based Multicomponent Materials for Durable and Safe Performance (KMM-NoE) under the contract no. NMP3-CT-2004-502243.

References

1. Steele, B. C. H. and Heinzel, A., Materials for fuel-cell technologies. *Nature*, 2001, **414**, 345–352.
2. Tu, H. and Stimming, U., Advances, aging mechanisms and lifetime in solid-oxide fuel cells. *J. Power Sources*, 2004, **127**, 284–293.
3. Badwal, S. P. S., Stability of solid oxide fuel cell components. *Solid State Ionics*, 2001, **143**, 39–46.
4. Minh, N. Q., Solid oxide fuel cell technology—features and applications. *Solid State Ionics*, 2004, **174**, 271–277.
5. Haile, S. M., Fuel cell materials and components. *Acta Mater.*, 2003, **51**, 5981–6000.
6. Wen, T.-L., Wang, D., Chen, M., Tu, H., Lu, Z., Zhang, Z., Nie, H. and Huang, W., Material research for planar SOFC stack. *Solid State Ionics*, 2002, **148**, 13–519.
7. Kurokawa, H., Kawamura, K. and Maruyama, T., Oxidation behavior of Fe–16Cr alloy interconnect for SOFC under hydrogen potential gradient. *Solid State Ionics*, 2004, **168**, 13–21.
8. Zhu, W. Z. and Deevi, S. C., Development of interconnect materials for solid oxide fuel cells. *Mater. Sci. Eng. A*, 2003, **348**, 227–243.
9. Antepara, I., Villarreal, I., Rodrıguez-Martınez, L. M., Lecanda, N., Castro, U. and Laresgoiti, A., Evaluation of ferritic steels for use as interconnects and porous metal supports in IT-SOFCs. *J. Power Sources*, 2005, **151**, 103–107.
10. Menzler, N. H., Sebold, D., Zahid, M., Gross, S. M. and Koppitz, T., Interaction of metallic SOFC interconnect materials with glass–ceramic sealant in various atmosphere. *J. Power Sources*, 2005, **152**, 156–167.
11. Fergus, J. W., Sealants for solid oxide fuel cells. *J. Power Sources*, 2005, **147**, 46–57.
12. Weil, K. S., The state-of-the-art in sealing technology for solid oxide fuel cells. *JOM*, 2006, 36–44.
13. Lara, C., Pascual, M. J. and Duran, A., Glass-forming ability, sinterability and thermal properties in the systems RO–BaO–SiO_2 (R = Mg, Zn). *J. Non-Cryst. Solids*, 2004, **348**, 149–155.

14. Bansal, N. P. and Gamble, E. A., Crystallization kinetics of a solid oxide fuel cell seal glass by differential thermal analysis. *J. Power Sources*, 2005, **47**, 107–115.
15. Yang, Z., Meinhardt, Kerry D. and Stevenson, J. W., Chemical compatibility of barium–calcium–aluminosilicate-based sealing glasses with the ferritic stainless steel interconnect in SOFCs. *J. Electrochem. Soc.*, 2003, **150**, A1095–A1101.
16. Lahl, N., Bahadur, D., Singh, K., Singheiser, L. and Hilpertz, K., Chemical interactions between aluminosilicate base sealants and the components on the anode side of solid oxide fuel cells. *J. Electrochem. Soc.*, 2002, **149**, A607–A614.
17. Batfalsky, P., Haanappel, V. A. C., Malzbender, J., Menzler, N. H., Shemet, V., Vinke, I. C. and Steinbrech, R. W., Chemical interaction between glass–ceramic sealants and interconnect steels in SOFC stacks. *J. Power Sources*, 2006, **155**, 128–137.
18. Brochu, M., Gauntt, B. D., Shah, R., Miyake, G. and Loehman, R. E., Comparison between barium and strontium–glass composites for sealing SOFCs. *J. Eur. Ceramic Soc.*, 2006, **26**, 3307–3313.
19. Bahadur, D., Lahl, N., Singh, K., Singheiser, L. and Hilpert, K., Influence of nucleating agents on the chemical interaction of $MgO–Al_2O_3–SiO_2–B_2O_3$ glass sealants with components of SOFCs. *J. Electrochem. Soc.*, 2004, **151**, A558–A562.
20. Krause, D., Thomas, B., Leinenbach, C., Eifler, D., Minay, E. J. and Boccaccini, A. R., The electrophoretic deposition of bioglass ®particles on stainless steel and nitinol substrates. *Surf. Coat. Technol.*, 2006, **200**, 4835–4845.
21. Larsen, P. H., The influence of SiO_2 addition to $2MgO–Al_2O_3–3.3P_2O_5$ glass. *J. Non-Cryst. Solids*, 1999, **244**, 16–24.
22. Li, W. and Mitchell, B., Nucleation and crystallization in calcium aluminate glasses. *J. Non-Cryst. Solids*, 1999, **255**, 199–207.
23. Francis, A. A., Rawlings, R. D., Sweeney, R. and Boccaccini, A. R., Crystallization kinetic of glass particles prepared from a mixture of coal ash and soda-lime cullet glass. *J. Non-Cryst. Solids*, 2004, **333**, 187–193.
24. Kissinger, H. E., *J. Res. Natl. Bur. Stand. (US)*, 1956, **57**(4), 217.
25. Boccaccini, A. R., Stumpfe, W. and Taplin, D. M. R., Densification and crystallization of glass powder compacts during constant heating rate sintering. *Mater. Sci. Eng. A*, 1996, **219**, 26–31.
26. Aloisi, M., Karamanov, A. and Pelino, M., Sintered glass–ceramic from municipal solid waste incinerator ashes. *J. Non-Cryst. Solids*, 2004, **345/346**, 192–196.